

Synthesis, Characterization, and Electrochemical Study of Novel Porphyrin Derivatives as Corrosion Inhibitors for Carbon Steel in HCl Solutions

Mohammed Thamer Jaafar¹, Luma Majeed Ahmed^{2*}, and Rahman Tama Haiwal²

¹Department of Petroleum Engineering, College of Engineering, University of Kerbala, Karbala 56001, Iraq

²Department of Chemistry, College of Science, University of Kerbala, Karbala 56001, Iraq

* **Corresponding author:**

email: luma.ahmed@uokerbala.edu.iq

Received: August 4, 2023

Accepted: October 4, 2023

DOI: 10.22146/ijc.87682

Abstract: This study involves the synthesis of some porphyrins derivatives, these are termed as 4,4',4'',4'''-(porphyrin-5,10,15,20-tetrayl)tetrakis(N-(6-aminoacridin-3-yl)benzamide) (**3a**), 4,4',4'',4'''-(porphyrin-5,10,15,20-tetrayl)tetrakis(N-(5-methoxybenzo[d]thiazol-2-yl)benzamide) (**3b**), 4,4'-(10,20-bis(3-hydroxyphenyl)porphyrin-5,15-diyl)bis(N-(6-aminoacridin-3-yl)benzamide) (**5a**), and 4,4'-(10,20-bis(3-hydroxyphenyl)porphyrin-5,15-diyl)bis(N-(benzo[d]thiazol-2-yl)benzamide) (**5b**). These derivatives were synthesized using open circuit potential (OCP) and potentiodynamic polarization (PDP) in 0.1 M HCl solution methods. These derivatives were characterized using nuclear magnetic resonance (¹H- and ¹³C-NMR) spectroscopy, mass spectra (ESI), and micro elemental analysis (CHN). The activity of these synthesized materials was investigated as a corrosion inhibitor using carbon steel (CS) as a model for corroded materials. The obtained results showed that the synthesized porphyrins derivatives were effective corrosion inhibitors to 0.1 M HCl solution for CS. In the case of the derivative **3a**, a maximum inhibition efficiency (IE%) was recorded and it was around 74%. The derivative **3b** showed an IE% of around 68.11%, while the %IE of **5a** and **5b** were around 18.98% and 45.16%, respectively. The best IE% value that was recorded for the derivative **3a** has the potential to be effective anticorrosive coatings for industrial applications and act as mixture inhibitor because their ΔE_{corr} values are less than 85 mV. On the CS surface following treatment with compound **3a**, the inhibitor mechanism for acidic medium (HCl) was investigated.

Keywords: amides derivative; carbon steel; corrosion; inhibition efficiency; porphyrin derivatives

■ INTRODUCTION

Carbon steel (CS) as a raw material, is one of the most important industrial materials in our modern world. It is made from an alloy of carbon, traces of other metals, and iron [1-2]. CS has excellent properties such as good mechanical, annealing, welding properties, and inexpensive [3]. Additionally, CS has been used in a variety of industries, including industry, oil, and gas [2,4-6]. Because of the severe impacts of the acid solutions that can be used as a solvent for dissolving the rocks in the oil well rocks, the CS utilized for oil exploration in wells may corrode. Acid solutions are used in many industrial fields to clean and descale steel substrates, remove mud, dissolve

rubble, and create channels in rocks for accessing crude oil flow [7]. The use of 5–28% HCl is thought to be the most common approach for improving the production of additional oil and gas worldwide [2,8].

Today, it is essential to prevent corrosion damage using a variety of techniques and approaches, like surface coating or using components that serve as corrosion inhibitors and cathodic protection, such as inorganic or organic substances. This is because the three key domains of economics, safety, and conservation are all affected by corrosion problems [9-12]. However, taking into account the truth in applying acidic solutions for different objectives, the inhibitor application is

considered one of the most efficient procedures that can be presented to suppress the corrosion process because it is readily practicable, effective, and economical [13].

Numerous different inorganic and organic substances have been employed to prevent corrosion in acidic corrosive media for CS [14]. Typically, inhibitors develop a compact protective or passive coating on the metal's surface after adhering to it to slow the rate of corrosion [15]. It has been discovered that organic compounds having N, S, and O heteroatoms, particularly when combined with electronic or aromatic systems, have strong anticorrosion potential [16]. The porphyrin molecule has the chemical structure of a possible corrosion inhibitor since it is an acid of the type of Lewis with a network of conjugated-electron systems and 4-nitrogen atoms at its center. It is a tetradentate chelating agent with strong bonding properties and a clear capacity to engage surfaces via a variety of chemical and/or physical processes [17].

Complexes of metal-porphyrin are adaptable models for metalloenzymes and electron transporting in biological media. Porphyrins are employed in a broad range of different procedures, such as ligands for the spectrophotometric detection of cations, stable phases in high-performance liquid chromatography (HPLC), photovoltaic cells, biosensors, membrane components, and catalysis, for electrodes of ion-selective [18-21]. They have also been used as CS corrosion inhibitors in aqueous mineral acids, according to reports [22-24]. According to multiple research on the corrosion prevention characteristics of various molecules of porphyrin, porphyrin molecules may alter the distribution of electrons for their rings of conjugated aromatic to produce layers of ordered molecular on the surface of the electrode [25-26]. These layers of molecules operate as a barrier to stop electroactive substances from diffusing toward the metal surface. Groups of peripheral functional, electron density, and steric hindrance donor centers are some of the variables that have an impact on the porphyrin molecules' adsorption and their ability to suppress corrosion [27]. However, very few articles have focused on its capacity to guard against iron corrosion up to this point [28-29].

The present study would aim to synthesize four different types of porphyrin derivatives (**3a**, **3b**, **5a**, and **5b**) and then create adlayers on CS by dipping an iron electrode into a solution of 0.1 M HCl acid, which included porphyrin molecules. These compounds' behavior would be screened as an efficient corrosion inhibitor on iron surfaces using electrochemical methods and the surfaces.

■ EXPERIMENTAL SECTION

Materials

In this study, reagent-grade starting compounds pyrrole, 4-formylbenzoic acid, sulfurous dichloride, 5-methoxybenzothiazol-2-amine, acridine-3,6-diamine, triethylamine, ethanol absolute, and HCl were purchased from Sigma-Aldrich and Merck. They were applied without more purification for the synthesis of the porphyrin derivative inhibitor and the corrosive medium.

Instrumentation

Different methods and techniques were used to characterize the chemical structures of the synthesized materials. Melting points were recorded using a digital Electro-Thermal Stuart SMP-30. Fourier transform infrared spectroscopy (FTIR) was recorded using Shimadzu FTIR-8400S. Nuclear magnetic resonance spectra were obtained in DMSO- d_6 using a Bruker spectrometer (500 MHz for $^1\text{H-NMR}$, 125 MHz for $^{13}\text{C-NMR}$). ESI-mass spectra were acquired using an Agilent Technology (HP) instrument (EI, 70 eV). Micro elemental analysis was conducted using a Heraeus CHN-O-Rapid analyzer.

Procedure

Synthesis of porphyrin derivative inhibitor

Synthesis of compound (3a, 3b). An amount of 4,4',4'',4'''(porphyrin-5,10,15,20-tetrayl)tetrabenzoic acid (TCPP) (7.907 g, 0.01 mol) was reacted with SOCl_2 (4.758 g, 0.04 mol) at ambient temperature and stirred at 70 rpm for 30 min. Following this, 5 mL of DMF was poured into the mixture and it was continuously stirred for 10 min at a constant temperature. The resulting

product was transmitted to a 25 mL round bottom flask with acridine-3,6-diamine (8.37 g, 0.04 mmol), and then 5-methoxybenzothiazol-2-amine (7.20 g) were added. The mixture of reaction was then refluxed at 120 °C for 2 h, and triethylamine (8.1 g, 0.08 mol) was subsequently added. The reaction mixture was further refluxed for 1 h at 120 °C. TLC (*n*-hexane: EtOAc) presented that the reaction was finished. The resulting black solution was quenched with ice crystals, filtered, and washed with ethanol. Then, it was recrystallized from ethanol and DMF, this procedure is modified from the method in reference [30].

The compound 4,4',4'',4'''-(porphyrin-5,10,15,20-tetrayl)tetrakis(*N*-(6-aminoacridin-3-yl)benzamide) (**3a**) was produced as a black powder with a yield of 70% and the melting point was above 350 °C. The FTIR spectrum (measured in KBr) presented in Fig. S1 showed peaks at 3333–3300 (NH₂), 3201 (NH), 3055 (C–H aromatic), 1693 (C=O), 1600 cm⁻¹ (C=N), and 1489 cm⁻¹ (C=C) [31]. The ¹H-NMR spectrum presented in Fig. S3 displayed signals at δ_H 10.47 (s, 4 CONH), 8.41–8.37 (m, 8 pyrrole-H), 8.10–7.19 (m, 44 Ar-H), 6.46 (s, 8 NH₂), and –2.94 ppm (s, 2 NHint). The ¹³C-NMR spectrum exhibited signals at δ_C: 98.64, 111.89, 115.82, 116.22, 116.47, 119.87, 121.01, 122.82, 12.83, 124.64, 127.78, 129.09, 129.51, 129.53, 129.61, 129.62, 131.23, 133.48, 137.82, 138.04, 138.22, 138.94, 139.76, 147.24, 174.42, 150.66, 159.00, 159.14, and 166.30 ppm. The calculated elemental composition for C₁₀₀H₆₆N₁₆O₄ was C 77.20%, H 4.28%, N 14.41%, and O 4.11%, which was consistent with the found composition of C 77.04%, H 4.10%, N 14.22%. The ESI-MS spectrum showed the calculated exact mass for (C₁₀₀H₆₆N₁₆O₄) to be 1555.55 and the found mass was 1555.50.

The compound 4,4',4'',4'''-(porphyrin-5,10,15,20-tetrayl)tetrakis(*N*-(5-methoxybenzo[d]thiazol-2-yl)benzamide) (**3b**) was produced as a black powder with a yield of 73% and a melting point was above 350 °C. The FTIR spectrum (KBr, cm⁻¹) presented in Fig. S2 showed peaks at 3441 (N–H), 3059 (C–H aromatic), 2924 (C–H aliphatic), 1693 (C=O), 1612 (C=N), 1454 (C=C), and 605 cm⁻¹ (C–S) [31]. The ¹H-NMR spectrum presented in Fig. S4 exhibited signals at δ_H (ppm) 10.46 (s, 4 CONH), 8.41–8.34 (m, 8 pyrrole-H), 8.22–7.30 (m, 28 Ar-H), 3.89 (s, 12

OCH₃), and –3.00 ppm (s, 2 NHint). The ¹³C-NMR spectrum presented in Fig. S5 displayed signals at δ_C: 60.14, 98.39, 113.61, 115.82, 116.22, 122.63, 122.82, 122.83, 126.76, 127.09, 127.78, 129.51, 129.53, 129.61, 129.62, 131.90, 137.82, 138.04, 138.22, 139.02, 150.74, 157.77, 159.02, 159.17, 161.55, and 166.50 ppm. The calculated elemental analysis for C₈₀H₅₄N₁₂O₈S₄ gave C 66.75, H 3.78, N 11.68, O 8.89, S 8.91, while the found percentages were C 66.65, H 3.36, and N 11.25%.

Synthesis of compound (5a, 5b). An amount of 4,4'-(10,20-bis(3-hydroxyphenyl)porphyrin-5,15-diyl)dibenzoic acid (7.41 g, 0.01 mol) was reacted with 2.4 g (0.02 mol) of SOCl₂ at ambient temperature and stirred at 70 rpm for 30 min. Next, 5 mL of DMF was used and the mixture was continuously stirred for an additional 10 min at a constant temperature. The resulting solution was transmitted to a 25 mL round bottom flask with acridine-3,6-diamine (4.18 g, 0.02 mmol), and then 3.60 g of 5-methoxybenzothiazol-2-amine was added. The reaction mixture was then refluxed at 120 °C for 2 h followed by the addition of triethylamine (Et₃N, 4.1 g, 0.04 mol). The mixture of reaction was returned for an additional hour at 120 °C. The resulting black solution was quenched with ice crystals, filtered, and washed with ethanol; this procedure is modified from the previously method [30].

4,4'-(10,20-bis(3-hydroxyphenyl) porphyrin-5,15-diyl)bis(*N*-(6-aminoacridin-3yl)benzamide) (**5a**) is a black powder with a yield of 65% and a melting point greater than 350 °C. The FTIR spectrum (KBr, cm⁻¹) presented in Fig. S6 shows peaks at 3414–3322 (NH₂), 3200–2400 (O–H), 3055 (C–H aromatic), 1701 (C=O), 1604 (C=N), and 1485 cm⁻¹ (C=C), as well as an N–H band at 1269 cm⁻¹. The ¹H-NMR spectrum presented in Fig. S8 shows signals at δ_H (ppm) 10.45 (s, 2 CONH), 8.69–8.35 (m, 8 pyrrole-H), 8.13–7.25 (m, 28 ArH), 7.05 (s, 2 OH), 6.81 (d, *J* = 1.4 Hz, 2H), 6.25 (s, 4NH₂), and –1.47 (s, 2 NH pyrrole) [32]. The calculated elemental analysis for C₇₂H₄₈N₁₀O₄ is C 77.40%, H 4.33%, N 12.54%, and O 5.73%, while the actual analysis shows C 77.25%, H 4.13%, and N 12.34%.

4,4'-(10,20-bis(3-hydroxyphenyl)porphyrin-5,15-diyl)bis(*N*-(benzo[d] thiazol-2-yl)benzamide) (**5b**). It is

Table 1. Materials chemical composition applied in the carbon steel specimens [8]

Element	C	Si	Mn	S	P	Cu	Ni	Cr	Fe
%	0.42	0.30	1.40	0.05	0.05	0.50	0.20	0.20	96.88

a black powder with a yield of 76% and a melting point was over 350 °C. Its FTIR spectrum, measured using KBr, presented in Fig. S7 shows peaks at 3406 (N–H), 3221–2400 (O–H), 3029 (C–H aromatic), 2947 (C–H aliphatic), 1701 (C=O), 1608 (C=N), 1485 (C=C), and 605 cm⁻¹ (C–S). Its ¹H-NMR spectrum presented in Fig. S9 shows peaks at δ_H (ppm) 10.68 (s, 2 CONH), 8.84–8.27 (m, 8 pyrrole-H), 8.14–7.28 (m, 20 Ar–H), 7.03 (s, 2 OH), 6.80 (d, *J* = 1.4 Hz, 2H), 3.66 (s, 6 OCH₃), and –1.47 (s, 2 NH pyrrole) [32]. Its calculated elemental composition is C 70.31%, H 4.00%, N 10.58%, O 9.06%, and S 6.05%, while the measured composition is C 70.15%, H 3.92%, N 10.32%, and S 6.00%.

Corrosion investigation of carbon steel

In this study, the used working electrodes were CS specimens obtained from a Metal Sample Company, with a composition as specified in Table 1 [8]. The used corrosive medium was a 0.1 M HCl solution (5 mL), prepared by diluting analytical grade 37% HCl (Sigma Aldrich) with double-distilled water. All the CS specimens utilized in this investigation had the following dimensions: 25 mm in diameter, 3 mm in height, and an effective area of 1 cm². Before each run, the specimen surfaces were mechanically polished using fine-grade emery paper (80/3000 grades), washed with double-distilled water, then degreased with acetone, dried, and stored in a desiccator.

The electrochemical reactions were monitored using a WENKING M Lab Bank Elektronik-Intelligent controls GmbH potentiostat, which was connected to a computer using an RS 232 cable. The M Lab potentiostat/galvanostat has three operational modes for each channel: potentiostats, galvanostatic, and open circuit. However, for this experiment, potentiodynamic polarization was performed in a three-electrode glass cell with a water jacket, including a corrosion cell with three electrodes. The working electrodes were made of CS, the counter electrode was made of platinum, and the reference electrode was made of silver-silver chloride.

Two sets of experiments were conducted on the CS specimens: without and with inhibitor at a concentration of 0.5 mmol, with a temperature of 292 K.

Tafel polarization measurement was performed by applying a potential ranging from approximately 200 mV to the open circuit voltage (OCP). The polarization curve experiments were started after immersing the working electrode in the solution for 30 min to reach steady state potential. Three measurements were performed, and only the average data were reported.

The corrosion current density (*i*_{corr}) and corrosion potential (*E*_c) values were calculated for all corrosion parameters. Additionally, the Tafel slopes, "β_a" and "β_c" were predicted using the linearity part of the cathodic and anodic curves, respectively [33–34]. The inhibitory efficiency (%IE) from the polarization investigation was computed using Eq. (1) [35–36];

$$\%IE = \frac{i_{\text{corr}} - i_{\text{corr},i}}{i_{\text{corr}}} \times 100 \quad (1)$$

where *i*_{corr*i*} and *i*_{corr} are the corrosion current densities with and without porphyrin derivative, respectively.

RESULTS AND DISCUSSION

Spectroscopic Characterization and Synthesis of the Porphyrin Derivatives

Synthesis and characterization of compounds 3a and 3b

Compound 1 was reacted with two different amines (acridine-3,6-diamine, and 5-methoxy benzo[d]thiazol-2-amine) to produce compounds 3a and 3b, as illustrated in Fig. 1. As presented in Fig. S1–S4, the presence of the amide group and absence of the carbonyl group were confirmed by infrared spectroscopy, which showed a peak at 3400 cm⁻¹. The presence of the amide group and absence of the carbonyl group in ¹H-NMR spectroscopy which showed a peak at about 10.47 ppm. The experimental section provides detailed information on the complete spectrum of all

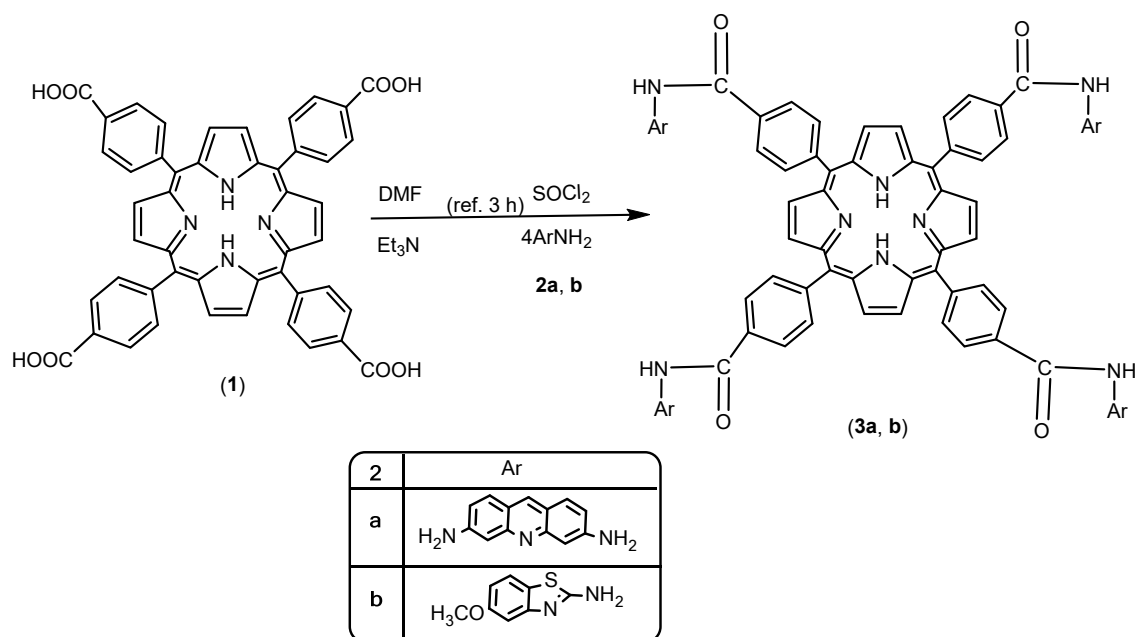


Fig 1. Schematic diagram of prepared compounds 3a and 3b

porphyrin derivatives, including ESI-MS, FTIR, $^1\text{H-NMR}$, and $^{13}\text{C-NMR}$, as well as their melting points. The identification of the new compounds was confirmed using various techniques, such as FTIR and $^1\text{H-NMR}$ spectroscopy. The appearance of the amide group and the disappearance of the OH peak in the carboxylic acid was observed in the infrared spectra of the synthesized compounds.

Synthesis and characterization of the compounds 5a and 5b

Compound 4 was undergone to react with two different amines, namely acridine-3,6-diamine and 5-methoxybenzo[d]thiazol-2-amine, resulting in the formation of compounds 5a and 5b, as explained in Fig. 2. The structural modifications in the synthesized compounds were confirmed through several analytical

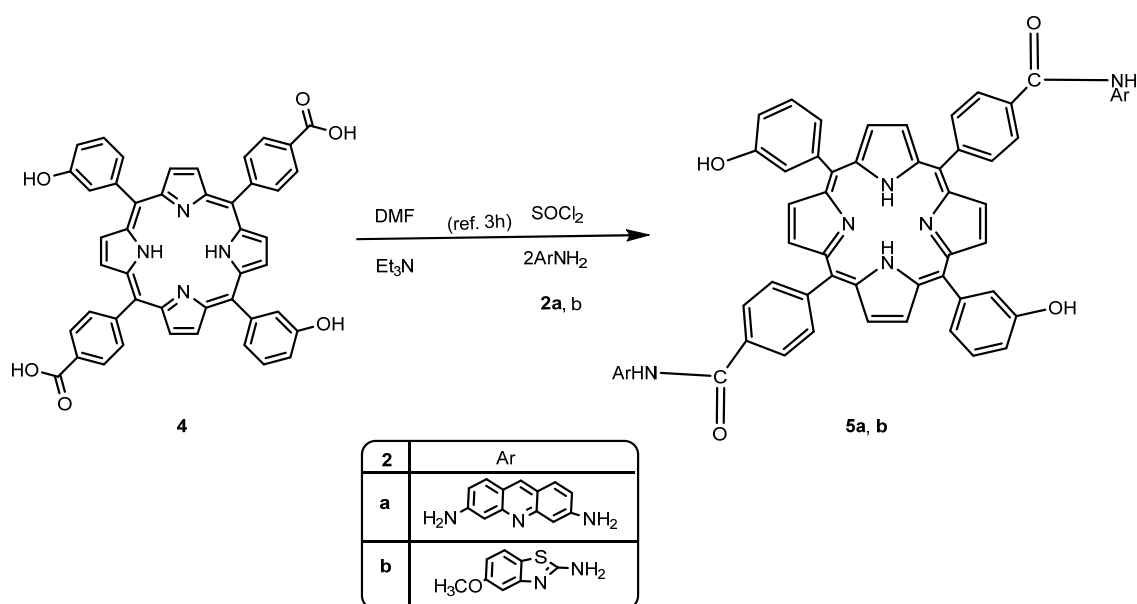


Fig 2. Schematic diagram of prepared compounds 3a and 3b

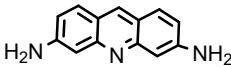
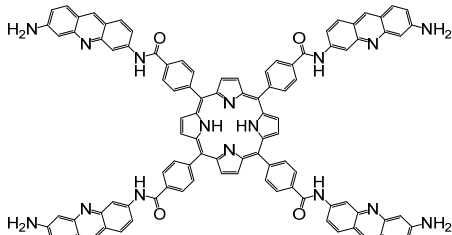
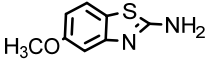
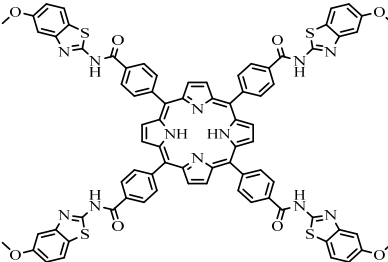
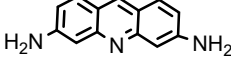
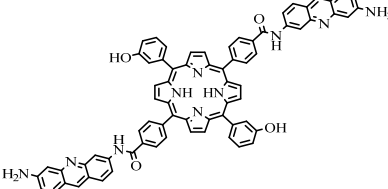
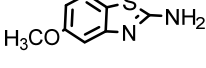
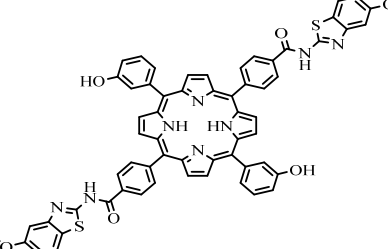
techniques, such as FTIR, ^1H and ^{13}C -NMR spectroscopy, and mass spectrometry. The infrared spectra in Fig. S5 and S6 displayed a characteristic peak at 3416 and 3406 cm^{-1} , indicating the presence of the amide group and the absence of the carbonyl group. Similarly, the ^1H -NMR spectra in Fig. S7 and S8 showed a peak at 10.45 and 10.68 ppm, indicating the presence of the amide group and the absence of the carbonyl group. Further confirmation of the synthesized compounds was obtained through FTIR and ^1H -NMR spectroscopy. The disappearance of the carboxylic acid OH peak and the appearance of the amide group in the infrared spectra confirmed the formation of the new compounds. The experimental section contains detailed information on the

complete spectrum of all porphyrin derivatives, including their melting points in Table 2.

Potentiodynamic Polarization

A CS sample submerged in a corrosive media in the presence and absence of the compounds **3a**, **3b**, **5a**, and **5b** at a temperature of 292 K, as shown in Fig. 3's polarization curves. There is a discernible difference in the Tafel area of a linear connection, and polarization curves between the logarithm of the current density and potential was discovered. Numerous electrochemical kinetic parameters for the corrosion process, including the corrosion current density (I_{corr}), corrosion potential (E_{corr}), and both anodic and cathodic Tafel slopes (c , a),

Table 2. Some of the physical characteristics and mass data of synthetic dyes

Entry	Amine	Product	Molecular formula	M.W. (g/mol)	Yield	Mass data (m/z) [M^+]
3a			$\text{C}_{100}\text{H}_{66}\text{N}_{16}\text{O}_4$	1555.74	70	1555.50
3b			$\text{C}_{80}\text{H}_{54}\text{N}_{12}\text{O}_8\text{S}_4$	1439.63	73	1438.31
5a			$\text{C}_{72}\text{H}_{48}\text{N}_{10}\text{O}_4$	1117.24	65	1116.39
5b			$\text{C}_{62}\text{H}_{42}\text{N}_8\text{O}_6\text{S}_2$	1059.19	76	1058.27

were calculated by extrapolating the anodic and cathodic areas of the Tafel lines. Table 3 has a list of these parameters.

Table 3 shows that the addition of compounds **3a**, **3b**, **5a**, and **5b** had a significant impact on the corrosion process compared to the blank solution. The difference in the ΔE_{corr} values for the prepared compounds was calculated using Eq. (2) [37-38] and demonstrated that all values are less than 85 mV. Hence, the inhibitor can be classified as an inhibitor mixture from cathodic or anodic inhibitors [35].

$$\Delta E_{\text{corr}} = E_{\text{corr,without inhibitor}} - E_{\text{corr,with inhibitor}} \quad (2)$$

Generally, the density of corrosion current (which is directly proportional to the rate of corrosion) of the sample minimized significantly after the addition of compounds **3a**, **3b**, **5a**, and **5b**. At 292 K, the corrosion current density of the blank solution was 0.3255 mA/cm² and decreased after the addition of the prepared compounds to a range of 0.0846–0.2637 mA/cm². When adding compound **3a**, the maximum depression in this value has occurred with a maximum value of %IE. This case is an attitude to include compound **3a** on four substituted aromatic amine groups in its structure symmetry compound. This aromatic amine group acts as an essential positive charge in organic inhibitors to control corrosion in an acidic medium [39]. Moreover, the addition of compounds **3b** and **5b** gives the medium value of %IE 68.11% and 45.16%, respectively. Because both contain heteroatoms in their structures, such as nitrogen, sulfur, and oxygen, these atoms include free pairs of electrons that support the link on the metal surface (mostly Fe and Cu) of CS by the adsorption method to produce a thin film layer. The formation of a

thin film layer will act as a barrier to separate the metal from the corrosive medium and block their active sites for acidic medium [40-42]. On the contrary, the addition of compound **5a** as anticorrosion involved less value of %IE, which may be an attitude to the big and asymmetric molecule, so its adsorption on CS is weak in the spirit of containing two amine groups substituted. Furthermore, the corrosion rate (CR) also declined with using prepared compounds.

In Fig. 3, overall, the polarization results indicate that the compounds **3a**, **3b** and **5a**, **5b** are effective in reducing the corrosion rate of CS in the tested conditions. The peak intensity for the blank is depressed after the addition of the prepared compounds and shifted the polarization curves towards a positive side during the formation of a thin layer onto the steel surface [43].

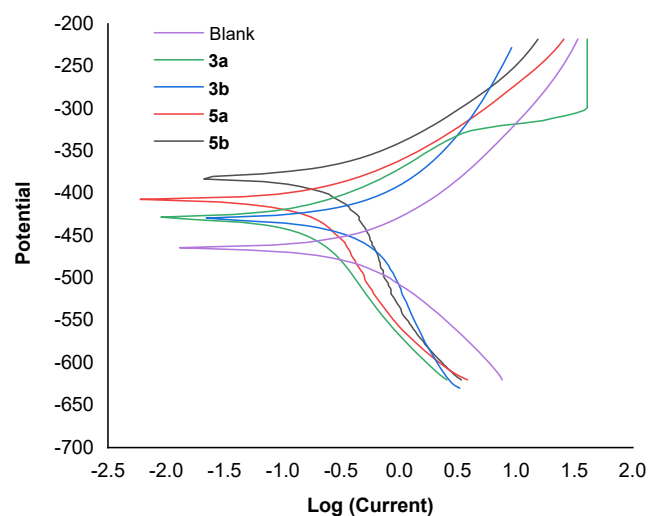


Fig 3. CS corrosion polarization curves in the absence and presence of chemicals **3a**, **3b**, **5a**, and **5b**

Table 3. Measurements of corrosion parameters for carbon steel using a Tafel scan in the presence and absence of compounds **3a**, **3b**, **5a**, and **5b** at temperature 292 K

Solution	T (K)	-E _{corr} (mV)	ΔE _{corr} (mV)	I _{corr} (mA/cm ²)	β _c (mV/dec)	Ba (mV/dec)	C.R (mm/y)	R _p (Ω/cm ²)	IE%
Blank	292	465.70	-	0.33	140	121	3.78	43.36	-
3a	292	429.10	36.60	0.08	185	76	0.98	138.70	74.00
3b	292	409.30	56.40	0.10	234	72	1.21	115.60	68.11
5a	292	430.60	35.10	0.26	293	124	3.06	71.85	18.98
5b	292	381.80	83.80	0.18	360	85	2.07	83.97	45.16

Mechanism of Inhibition

In terms of the inhibition process, it is commonly accepted that the initial stage of the inhibitors' action mechanism in hostile acid media is their adsorption at the metal solution interface. The porphyrin derivatives' ability to inhibit CS in an HCl solution may be explained in terms of adsorption. At the interface of metal-solution, organic molecules may adsorb in one of four ways [44]: First, through the attraction of electrostatics between the metal and charged molecules, the second is through interactions between the metal and electrons, third through interactions between the pairs of uncharged electrons within the molecule and the metal and the last one through a collection of the above.

The significant delocalization of the electrons in the porphyrin molecule, the unoccupied *d*-orbitals of the iron surface atoms, and the lone pairs of the heteroatoms make it clear that the direct adsorption of these elements on the Fe surface might take place [45]. Additionally, the density of electrons on the heterocyclic ring is increased by the electron presence-releasing additional NH₂ groups in the molecules. These substances may exist as protonated species in acidic solutions. These protonated species may adhere to the cathodic sites on the surface of CS and reduce hydrogen evolution. These substances' N atoms of heterocyclic and aromatic rings, as well as all electron-donating groups, allow them to adhere to anodic surfaces. These substances may lessen the anodic breakdown of CS by adhering to anodic sites. Two distinct methodologies were utilized to examine the inhibitory impact of the various chemicals used in this experiment. It is possible for heteroatoms with lone pairs of electrons to transfer their lone pairs of electrons into the *d*-orbitals of the surface iron atoms, which results in chemisorption [46]. Further oxidation of the surface iron atoms produces electrons that are consumed by NH-H⁺, causing the adsorbed cationic inhibitor molecules to return to their neutral form as shown in Eq. (3-4). Stronger chemical interactions are between the surface and inhibitor as shown in Fig. 4 [47].

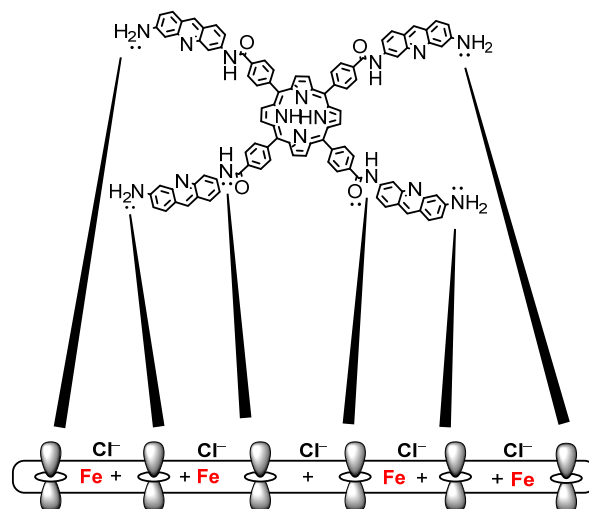
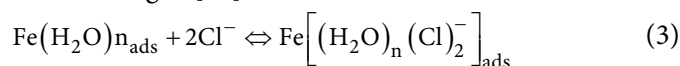
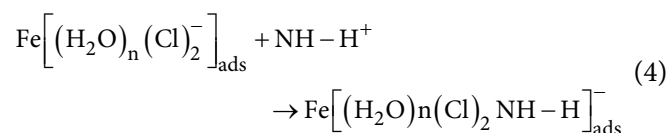


Fig 4. Illustration of the adsorptions of organic corrosion inhibitors compound **3a**



CONCLUSION

In this work, the easy preparation and costly effecting of new porphyrin derivatives **3a**, **3b**, **5a**, and **5b** were synthesized and characterized by applying different techniques of spectrophotometric. The synthesized materials were investigated as anti-corrosive materials by their doping over the CS surface. From this study, synthesized porphyrins derivatives were good inhibitors for CS in an acidic medium (0.1 M HCl). The derivatives **3a** and **3b** showed maximum values of inhibitor efficiency. All the differences in the ΔE_{corr} values for the compounds **3a**, **3b**, **5a**, and **5b** are less than 85 mV. All compounds (**3a**, **3b**, **5a**, and **5b**) can be classified as an inhibitor mixture from cathodic or anodic inhibitors. The compounds that contain amine groups or heteroatoms such as O, N, and S are more active in the surface protection of carbon steel in acidic media.

ACKNOWLEDGMENTS

The authors gratefully acknowledge all personnel who support this manuscript in the Faculty of Science and Faculty of Engineering at the University of Kerbala,

Department of Chemistry and the Department of Petroleum Engineering.

■ AUTHOR CONTRIBUTIONS

The theory part of this work was performed by Mohammed Thamer Jaafar and revised by Luma Majeed Ahmed and Rahman Tama Haiwal. The practical part and discussion were performed by Mohammed Thamer Jaafar and revised by Luma Majeed Ahmed. All authors agreed to the final version of this manuscript.

■ REFERENCES

- [1] Fouda, A.S., Megahed, H.E., Fouad, N., and Elbahrawi, N.M., 2016, Corrosion inhibition of carbon steel in 1 M hydrochloric acid solution by aqueous extract of *Thevetia peruviana*, *J. Bio- Tribo-Corros.*, 2 (3), 16.
- [2] Avdeev, Y.G., Nenasheva, T.A., Luchkin, A.Y., Marshakov, A.I., and Kuznetsov, Y.I., 2023, Thin 1,2,4-triazole films for the inhibition of carbon steel corrosion in sulfuric acid solution, *Coatings*, 13 (7), 1221.
- [3] Dwivedi, D., Lepková, K., and Becker, T., 2017, Carbon steel corrosion: A review of key surface properties and characterization methods, *RSC Adv.*, 7 (8), 4580–4610.
- [4] Fukaya, Y., and Watanabe, Y., 2018, Characterization and prediction of carbon steel corrosion in diluted seawater containing pentaborate, *J. Nucl. Mater.*, 498, 159–168.
- [5] Zhang, K., Xu, B., Yang, W., Yin, X., Liu, Y., and Chen, Y., 2015, Halogen-substituted imidazoline derivatives as corrosion inhibitors for mild steel in hydrochloric acid solution, *Corros. Sci.*, 90, 284–295.
- [6] Popoola, L.T., Grema, A.S., Latinwo, G.K., Gutti, B., and Balogun, A.S., 2013, Corrosion problems during oil and gas production and its mitigation, *Int. J. Ind. Chem.*, 4 (1), 35.
- [7] Onyeachu, I.B., Solomon, M.M., Umoren, S.A., Obot, I.B., and Sorour, A.A., 2020, Corrosion inhibition effect of a benzimidazole derivative on heat exchanger tubing materials during acid cleaning of multistage flash desalination plants, *Desalination*, 479, 114283.
- [8] Al-Najjar, S.S., and Al-Baitai, A.Y., 2022, Synthesized of novel imidazole-derived Schiff base as a corrosion inhibitor of carbon steel in acidic medium supported by electrochemical and DFT studies, *Phys. Chem. Res.*, 10 (2), 179–194.
- [9] de Araújo Macedo, R.G.M., do Nascimento Marques, N., Tonholo, J., and de Carvalho Balaban, R., 2019, Water-soluble carboxymethyl chitosan used as corrosion inhibitor for carbon steel in saline medium, *Carbohydr. Polym.*, 205, 371–376.
- [10] Wei, W., Geng, S., Xie, D., and Wang, F., 2019, High temperature oxidation and corrosion behaviours of Ni-Fe-Cr alloys as inert anode for aluminum electrolysis, *Corros. Sci.*, 157, 382–391.
- [11] Ijaola, A.O., Farayibi, P.K., and Asmatulu, E., 2020, Superhydrophobic coatings for steel pipeline protection in oil and gas industries: A comprehensive review, *J. Nat. Gas Sci. Eng.*, 83, 103544.
- [12] Fonseca, A.C., Lopes, I.M., Coelho, J.F., and Serra, A.C., 2015, Synthesis of unsaturated polyesters based on renewable monomers: Structure/properties relationship and crosslinking with 2-hydroxyethyl methacrylate, *React. Funct. Polym.*, 97, 1–11.
- [13] Ansari, K.R., Chauhan, D.S., Singh, A., Saji, V.S., and Quraishi, M.A., 2020, “Corrosion Inhibitors for Acidizing Process in Oil and Gas Sectors” in *Corrosion Inhibitors in the Oil and Gas Industry*, Eds. Saji, V.S., and Umoren, S.A., Wiley-VCH, Weinheim, Germany, 151–176.
- [14] Migahed, M.A., El-Rabiei, M.M., Nady, H., Gomaa, H.M., and Zaki, E.G., 2017, Corrosion inhibition behavior of synthesized imidazolium ionic liquids for carbon steel in deep oil wells formation water, *J. Bio- Tribo-Corros.*, 3 (2), 22.
- [15] Ahamad, I., Prasad, R., and Quraishi, M.A., 2010, Thermodynamic, electrochemical and quantum chemical investigation of some Schiff bases as corrosion inhibitors for mild steel in hydrochloric acid solutions, *Corros. Sci.*, 52 (3), 933–942.
- [16] Mashuga, M.E., Olasunkanmi, L.O., Adekunle, A.S., Yesudass, S., Kabanda, M.M., and Ebenso, E.E., 2015, Adsorption, thermodynamic and quantum chemical studies of 1-hexyl-3-methylimidazolium

- based ionic liquids as corrosion inhibitors for mild steel in HCl, *Materials*, 8 (6), 3607–3632.
- [17] Longo, F.R., De Luccia, J.J., and Agarwala, V.S., 1984, *Porphyrins as Corrosion Inhibitors*, Final Report, Naval Air Development Center, Warminster, Pennsylvania, US.
- [18] Lokesh, K.S., De Keersmaecker, M., and Adriaens, A., 2012, Self assembled films of porphyrins with amine groups at different positions: Influence of their orientation on the corrosion inhibition and the electrocatalytic activity, *Molecules*, 17 (7), 7824–7842.
- [19] Biesaga, M., Pyrzyńska, K., and Trojanowicz, M., 2000, Porphyrins in analytical chemistry. A review, *Talanta*, 51 (2), 209–224.
- [20] Xiao, J., and Meyerhoff, M.E., 1996, Retention behavior of amino acids and peptides on protoporphyrin-silica stationary phases with varying metal ion centers, *Anal. Chem.*, 68 (17), 2818–2825.
- [21] Guan, Z., Li, H., Wei, Z., Shan, N., Fang, Y., Zhao, Y., Fu, L., Huang, Z., Humphrey, M.G., and Zhang, C., 2023, Enhanced nonlinear optical performance of perovskite films passivated by porphyrin derivatives, *J. Mater. Chem. C*, 11 (4), 1509–1521.
- [22] Srivastava, M., 2023, Chemical facets of environment-friendly corrosion impediment of low-carbon steel in aqueous solutions of inorganic mineral acid, *Sci. Temper*, 14 (2), 284–287.
- [23] Furtado, L.B., Leoni, G.B., Nascimento, R.C., Santos, P.H.C., Henrique, F.J., Guimaraes, M.J.O.C., and Brasil, S.L.D.C., 2023, Experimental and theoretical studies of tailor-made Schiff bases as corrosion inhibitors for carbon steel in HCl, *Mater. Res.*, 26, e20220398.
- [24] Orozco-Agamez, J., Alviz-Meza, A., Kafarov, V., Colpas, F., Jimenez, M., and Pena-Ballesteros, D., 2023, Natural polymers as green corrosion inhibitors in carbon steels for applications in acid environment, *Chem. Eng. Trans.*, 100, 109–114.
- [25] Benmahammed, I., Douadi, T., Issaadi, S., Al-Noaimi, M., and Chafaa, S., 2020, Heterocyclic Schiff bases as corrosion inhibitors for carbon steel in 1 M HCl solution: Hydrodynamic and synergetic effect, *J. Dispersion Sci. Technol.*, 41 (7), 1002–1021.
- [26] Fratilesco, I., Lascu, A., Taranu, B.O., Epuran, C., Birdeanu, M., Macsim, A.M., Tanasa, E., Vasile, E., and Fagadar-Cosma, E., 2022, One A3B porphyrin structure—Three successful applications, *Nanomaterials*, 12 (11), 1930.
- [27] Jayaprakash, G.K., Kumara Swamy, B.E., Rajendrachari, S., Sharma, S.C., and Flores-Moreno, R., 2021, Dual descriptor analysis of cetylpyridinium modified carbon paste electrodes for ascorbic acid sensing applications, *J. Mol. Liq.*, 334, 116348.
- [28] Wolfram, A., Tariq, Q., Fernández, C.C., Muth, M., Gurrath, M., Wechsler, D., Franke, M., Williams, F.J., Steinrück, H.P., Meyer, B., and Lytken, O., 2022, Adsorption energies of porphyrins on MgO(100): An experimental benchmark for dispersion-corrected density-functional theory, *Surf. Sci.*, 717, 121979.
- [29] Singh, A., Lin, Y., Quraishi, M.A., Olasunkanmi, L.O., Fayemi, O.E., Sasikumar, Y., Ramaganthan, B., Bahadur, I., Obot, I.B., Adekunle, S.A., Kabanda, M.M., and Ebenso, E.E., 2015, Porphyrins as corrosion inhibitors for N80 steel in 3.5% NaCl solution: Electrochemical, quantum chemical, QSAR and Monte Carlo simulations studies, *Molecules*, 20 (8), 15122–15146.
- [30] Leggio, A., Belsito, E.L., De Luca, G., Di Gioia, M.L., Leotta, V., Romio, E., Siciliano, C., and Liguori, A., 2016, One-pot synthesis of amides from carboxylic acids activated using thionyl chloride, *RSC Adv.*, 6 (41), 34468–34475.
- [31] Jaafar, M.T., Ahmed, L.M., and Haiwal, R.T., 2023, Synthesis of novel porphyrin derivatives and investigate their application in sensitized solar cells, *Iraqi J. Chem. Pet. Eng.*, 24 (2), 113–122.
- [32] Kotteswaran, S., Mohankumar, V., Pandian, M.S., and Ramasamy, P., 2017, Effect of dimethylaminophenyl and thienyl donor groups on Zn-Porphyrin for dye sensitized solar cell (DSSC) applications, *Inorg. Chim. Acta*, 467, 256–263.
- [33] Hussien, H., Shahen, S., Abdel-karim, A.M., Ghayad, I.M., El-Shamy, O.A.A., Mostfa, N., and Ahmed, N.E.D., 2023, Experimental and theoretical evaluations: Green synthesis of new organic

- compound bis ethanethiyl oxalamide as corrosion inhibitor for copper in 3.5% NaCl, *Egypt. J. Chem.*, 66 (3), 189–196.
- [34] Deyab, M.A., Mele, G., Al-Sabagh, A.M., Bloise, E., Lomonaco, D., Mazzetto, S.E., and Clemente, C.D., 2017, Synthesis and characteristics of alkyd resin/M-porphyrins nanocomposite for corrosion protection application, *Prog. Org. Coat.*, 105, 286–290.
- [35] Khalib, A.A.K., Al-Hazam, H.A.J., and Hassan, A.F., 2022, Inhibition of carbon steel corrosion by some new organic 2-hydro-selenoacetamide derivatives in HCl medium, *Indones. J. Chem.*, 22 (5), 1269–1281.
- [36] Salleh, N.I.H., and Abdullah, A., 2019, Corrosion inhibition of carbon steel using palm oil leaves extract, *Indones. J. Chem.*, 19 (3), 747–752.
- [37] Verma, D.K., Ebenso, E.E., Quraishi, M.A., and Verma, C., 2019, Gravimetric, electrochemical surface and density functional theory study of acetohydroxamic and benzohydroxamic acids as corrosion inhibitors for copper in 1 M HCl, *Results Phys.*, 13, 102194.
- [38] Dagdag, O., El Harfi, A., Cherkaoui, O., Safi, Z., Wazzan, N., Guo, L., Verma, C., Ebenso, E.E., and Jalgham, R.T.T., 2019, Rheological, electrochemical, surface, DFT and molecular dynamics simulation studies on the anticorrosive properties of new epoxy monomer compound for steel in 1 M HCl solution, *RSC Adv.*, 9 (8), 4454–4462.
- [39] Roberge, P.R., 2019, *Handbook of Corrosion Engineering*, 3rd Ed., McGraw-Hill Education, New York, US.
- [40] Desai, P.D., Pawar, C.B., Avhad, M.S., and More, A.P., 2023, Corrosion inhibitors for carbon steel: A review, *Vietnam J. Chem.*, 61 (1), 15–42.
- [41] Lgamri, A., Abou El Makarim, H., Guenbour, A., Ben Bachir, A., Aries, L., and El Hajjaji, S., 2003, Electrochemical study of the corrosion behaviour of iron in presence of new inhibitor in 1 M HCl, *Prog. Org. Coat.*, 48 (1), 63–70.
- [42] Vinutha, M.R., and Venkatesha, T.V., 2016, Review on mechanistic action of inhibitors on steel corrosion in acidic media, *Port. Electrochim. Acta*, 34 (3), 157–184.
- [43] Alesary, H.F., Ismail, H.K., Shiltagh, N.M., Alattar, R.A., Ahmed, L.M., Watkins, M.J., and Ryder, K.S., 2020, Effects of additives on the electrodeposition of ZnSn alloys from choline chloride/ethylene glycol-based deep eutectic solvent, *J. Electroanal. Chem.*, 874, 114517.
- [44] Elewady, G.Y., 2008, Pyrimidine derivatives as corrosion inhibitors for carbon-steel in 2M hydrochloric acid solution, *Int. J. Electrochem. Sci.*, 3 (10), 1149–1161.
- [45] Muralidharan, S., Quraishi, M.A., and Iyer, S.V.K., 1995, The effect of molecular structure on hydrogen permeation and the corrosion inhibition of mild steel in acidic solutions, *Corros. Sci.*, 37 (11), 1739–1750.
- [46] Verma, C., Lgaz, H., Verma, D.K., Ebenso, E.E., Bahadur, I., and Quraishi, M.A., 2018, Molecular dynamics and Monte Carlo simulations as powerful tools for study of interfacial adsorption behavior of corrosion inhibitors in aqueous phase: A review, *J. Mol. Liq.*, 260, 99–120.
- [47] Chen, L., Lu, D., and Zhang, Y., 2022, Organic compounds as corrosion inhibitors for carbon steel in HCl solution: A comprehensive review, *Materials*, 15 (6), 2023.